Journal of
Composites Science

MDPI

Article

Improvement of Age-Resistance of LDPE-Based Nanocomposite Films by Addition of a Modified Layered Double Hydroxide with an Anionic UV Screener

Fuensanta Monzó [1], Alejandro Arribas [1], Francisco José Carrión-Vilches [2] and Ramón Pamies [2,*]

[1] Centro Tecnológico del Calzado & Plástico, 30840 Alhama de Murcia, Spain; f.monzo@ctcalzado.org (F.M.); a.arribas@ctcalzado.org (A.A.)
[2] Grupo de Ciencia de Materiales e Ingeniería Metalúrgica, Universidad Politécnica de Cartagena, Campus de la Muralla del Mar, 30202 Cartagena, Spain; fjc.vilches@upct.es
* Correspondence: ramon.pamies@upct.es

Abstract: In this study, we prepared plastic films composed of modified layered double hydroxides (LDHs), which were incorporated into a low-density polyethylene (LDPE) matrix. The sunscreen additive sulfonic phenylbenzimidazole acid sodium salt was incorporated as counter-anion in the interlayer of a nanoclay by means of ion-exchange reactions to improve thermal and optical properties. The modified LDHs were characterized using FT-IR, XRF, TGA, and XRD techniques. Cast extrusion was employed to obtain the nanocomposites with the new LDH incorporated into LDPE. The mechanical, rheological, and optical properties of the films were assessed, and the influence of a non-ionic surfactant was also evaluated. In addition, accelerated ageing tests were carried out to evaluate the influence of UV light on the mechanical and optical properties of the films.

Keywords: LDH; nanocomposites; LDPE; UV-ageing; photostability

check for updates

Citation: Monzó, F.; Arribas, A.; Carrión-Vilches, F.J.; Pamies, R. Improvement of Age-Resistance of LDPE-Based Nanocomposite Films by Addition of a Modified Layered Double Hydroxide with an Anionic UV Screener. *J. Compos. Sci.* **2023**, *7*, 388. https://doi.org/10.3390/jcs7090388

Academic Editor: Francesco Tornabene

Received: 31 August 2023
Revised: 8 September 2023
Accepted: 12 September 2023
Published: 14 September 2023

1. Introduction

In recent decades, a great deal of attention has been focused on the addition of inorganic layered materials to thermoplastic matrices to prepare new nanocomposites with higher compatibility between the inorganic filler and the organic polymer [1]. Layered double hydroxides (LDH) are a type of anionic clay, which are able to intercalate not only different kinds of additives, but also the polymeric chains of the nanocomposite [2]. The physical properties of LDH/polymer nanocomposites have been significantly improved recently [3,4]. The use of layered nanofillers as reinforcements in plastic materials increases flammability resistance and improves modulus impact strength and barrier properties of the resultant composite material [5–7].

The type and ratio of divalent and trivalent metal ions and the nature of the intercalated anion are key factors that can be adjusted and exert a major influence on the properties of the layered double hydroxide material. The LDH general formula is $[M^{2+}_{1-x}M^{3+}_{x}(OH)_2]A^{n-}_{x/n}\cdot mH_2O$, where M is a transition metal such as divalent and trivalent cations, and A is an interlayer inorganic anion [8]. LDHs are positively charged by the brucite-like sheets that are balanced by anions placed in the interlayers to ensure the electroneutrality of the material. Specifically, when the nanoclays contain Mg and Al sheets with CO_3^{2-} anions, these LDHs are usually called hydrotalcites. Recently, the ability of LDHs to exchange the counter anions has caught the attention of the scientific community. LDH host layers improve the thermal and optical stabilization of the exchanged anions. This feature opens the possibility of these materials progressing the development of promising applications in different fields such as wastewater clarification [9], biomedicine [10], and polymer additives [11,12], among others [13].

Melt mixing is the preferred method for the preparation of polymer composites modified with LDH because of the absence of monomers and solvents. Therefore, it is an

easy, economical, and environmentally friendly technique for the manufacturing of nano- and microcomposites. Furthermore, the major deformation and energy employed during extrusion improve the dispersion of the nanomaterial into the thermoplastic material [14]. The dispersion of nanoclays into plastic matrices is a technological challenge as the lack of polarity of the polymeric backbone complicates the homogeneous dispersion of the platelets. Thus, the addition of compatibilizers is a widely used strategy to favor the exfoliation of hydrotalcite-like particles [15].

Polyethylene is a plastic that is broadly used in many different domestic and industrial applications, with three different structures depending on the degree of ramification of the polymeric chain: high-density polyethylene (HDPE), linear low-density polyethylene (LLDPE), and low-density polyethylene (LDPE). From the structural point of view, LDPE has the most branching with lower intermolecular forces, which causes higher flexibility. This plastic is especially used in the manufacturing of disposable bags, packaging, and greenhouse applications. UV irradiation [16], thermo-oxidation [17], and chemical oxidation [18] are the most common degradation mechanisms of polyethylene, which is a non-biodegradable plastic that causes environmental problems [19]. For outdoor applications, polyethylene-based materials suffer from photodegradation. The atmosphere filters the sunlight, but UV radiation (290–400 nm) affects the stability of polyolefin plastics due to the presence of catalyzers and/or the different additives used in manufacturing. Therefore, UV light can affect the service life of polyethylene, so the use of sunscreen additives is necessary [20].

We have previously evaluated the addition of a modified LDH to LDPE matrix to improve the optical properties of the composite [21]. Based on that, we now explore the influence of the addition of sulfonic phenylbenzimidazole acid sodium salt (PBS), focusing on the effect of accelerated UV-aging of LDPE. Although PBS is a widely used sunscreen protector [22,23], this is the first time that its usage as an additive in polymeric matrix has been explored, to the best of our knowledge. This is due to its low dispersibility in non-polar materials and thermal degradation during the fabrication of films. Via ion-exchange reaction, this anion replaced the counter carbonate anions of an Mg-Al-based layered double hydroxide. The objective of the encapsulation is better compatibility with LDPE and thermal stabilization of PBS. Films of the new composites were manufactured by extrusion. LDPE with the addition of neat PBS and PBS-modified LDH were examined, as was the usage of a non-ionic surfactant.

The aim of the study is to obtain a sunscreen additive composed of PBS encapsulated in LDH with enhanced thermal and optical properties, which is able to improve the UV-light resistance of LDPE. With this strategy, we also improve the distribution in the polymeric matrix and immobilize the additive to avoid migration and exudation. Then, the sunscreen protection can be reached at low values of concentration with the potential to extend the lifetime of LDPE and reduce plastic waste.

2. Materials and Methods

The thermoplastic matrix for the preparation of the new composites was low-density polyethylene (LDPE). The neat plastic, labelled "LPDE Alcudia PE003" and produced by high-pressure autoclave technology, was purchased by Repsol Technology Centre. Kysuma Chemicals provided the layered double hydroxide with reference HT4AU. According to the supplier, this nanoclay has the formula $Mg_4Al_2(OH)_{12}(CO_3)\cdot nH_2O$, with a particle size of 0.4 µm and a monovalent anionic exchange capacity of 4.2 mmol/g.

Sulfonic phenylbenzimidazole acid sodium salt (PBS) was employed as a UV absorber, with the molecular structure depicted in Scheme 1a. This additive was supplied by Chemspec Chemicals, with CAS number 5997-53-5. This chemical is used in sunscreen applications, and it has UV-B radiation absorption with a maximum of 302 nm. It presents a solubility of 24 g/L in water at 25 °C [24]. To improve the dispersion of the additives in the thermoplastic matrix, sorbitan monostearate (SPAN60), with CAS number 1338-41-6, was added. The formula of this hydrophobic surfactant is shown in Scheme 1b.

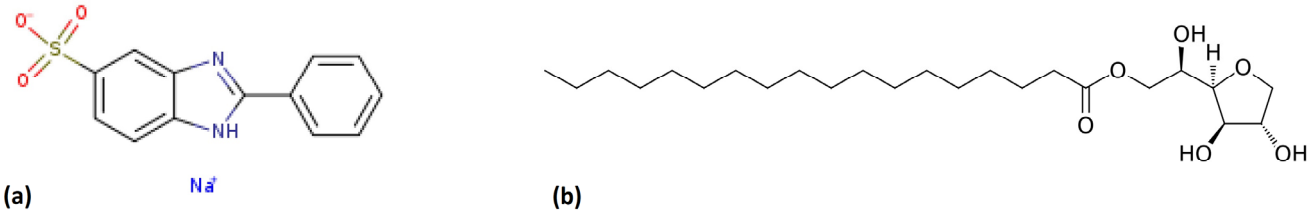

Scheme 1. (**a**) Chemical structure of PBS and (**b**) SPAN 60.

In order to determine the elemental composition of the modified LDH, a Leco CHN628 analyzer was employed (Leco Corporation, Benton Harbor, MI, USA). Bruker S4 Pioneer equipment was utilized for the X-ray fluorescence (XRF) characterization. The thermogravimetric analyses (TGA) were carried out by means of Mettler Toledo TGA/SDTA 851e/LF1100 equipment. The X-ray diffraction patterns were recorded in a Bruker D-8 Advance diffractometer using a wavelength of 1.542 Å from Cu Kα, with an angular speed of 120 °/s, at room temperature.

The preparation of neat LDPE films and the analogous films with additives involved a premixture and predispersion in a Leistritz ZSE 18HP 40D compounding extruder with intermeshed co-rotating screws, and a cast film extrusion line was used to obtain the films with a Dr. Collin E20P single-screw extruder. Technical data of the extruder and the processing conditions can be found in Table 1.

Table 1. Technical characteristics of the extruder and extrusion conditions of the films.

L/D Ratio	Diameter	Die Width	Calender Width	Speed	Die Pressure
25 mm	20 mm	100 mm	220 mm	60 rpm	45 bares
Temperature ramp					
Feeding	Zone 1	Zone 2	Zone 3	Zone 4	Die
35 °C	200 °C	208 °C	209 °C	185 °C	190 °C

The viscoelastic performance of the new composites was determined with a DHR1 rotational rheometer (TA Instruments; New Castle, DE, USA) with a configuration of parallel plates at 190 °C. The strain was set to 1% after the determination of the linear viscoelastic region, and angular frequency sweeps were performed in a range between 0.1 and 200 s^{-1}. The mechanical behavior of the samples was tested in a universal test machine ProLine Z010 from Zwick/Roell using a contact extensometer, in accordance with UNE-EN ISO 527-1: 2020 and UNE-EN ISO 527-3:2019 standards.

UV–visible spectra were evaluated with a Perkin Elmer Lambda 750S UV–Vis spectrophotometer. The absorbance of the films was recorded in the range from 200 to 800 nm. In order to evaluate the resistance of the films to the action of UV light, a xenon-accelerated weathering chamber was used. The samples were placed in an Atlas Suntest XSL+ chamber with irradiation (300–400 nm) = 60 ± 2 W/m^2 and a Black Standard Temperature (BST) of 65 ± 3 °C, as per the UNE-EN ISO 4892-2:2006 standard.

3. Results

3.1. Encapsulation of the UV Absorber and Characterisation of the Modified LDH

3.1.1. Intercalation of PBS in LDH and Determination of the Composition of PBS-LDH

LDHs are known to have the highest affinity to carbonate anions and are thus commonly used as anion-exchangeable compounds. In this case, we have prepared a precursor to facilitate the introduction of the UV absorber. Firstly, a simple anion exchange reaction was used to replace the carboxylate anions by chloride anions, as described by Iyi et al. [25], and obtain the chloride-LDH (Cl-LDH) precursor with larger basal interspace. Then, by means of a second ionic exchange reaction, PBS replaced chloride anions and a modified

LDH was obtained with PBS as intercalated anions (PBS-LDH). XRF and CHNS analyses were carried out to calculate the composition of the new PBS-LDH and compared to Cl-LDH and PBS-LDH. These data are presented in Table 2, showing an effective replacement of the anions.

Table 2. Concentration of the elements of the modified LDH determined by XRF and CHNS analyses.

	Concentration (wt. %)	
Elements	**Cl-LDH**	**PBS-LDH**
Na	2.03	0.775
Mg	13.55	6.89
Al	14.63	5.88
S	0.058	5.51
C	0.34	27.64
Cl	14.73	1.08
H	3.70	5.42
N	-	4.95

3.1.2. FT-IR Spectroscopy Characterization of the New PBS-LDH

We have also carried out FT-IR tests to confirm the incorporation of PBS into LDH. Figure 1 shows the normalized intensity of the FT-IR spectra of PBS, chloride-LDH, and PBS-LDH. Neat PBS presents a peak at 1190 cm^{-1}, ascribed to the asymmetric stretches of the sulfonate group [26]. The symmetric stretching vibrations of the group correspond to the wavenumbers from 1030 cm^{-1} to 1090 cm^{-1}. When PBS is added to LDH, these peaks are clearly seen at 1026, 1086, and 1188 cm^{-1}. This indicates that PBS was incorporated into LDH. The N-H hydrogen bonding of the imidazolium and the O-H stretching vibrations originate broader peaks, which were seen from 2950 cm^{-1} to 3550 cm^{-1} [27–29].

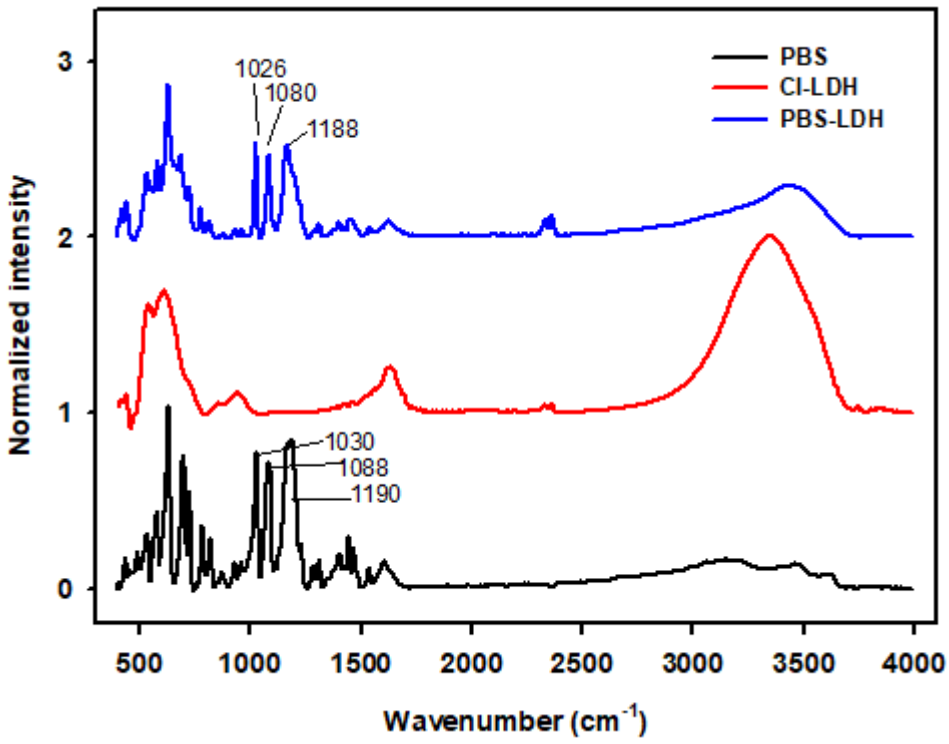

Figure 1. FT-IR spectra of neat PBS and the modified LDHs: Cl-LDH and PBS-LDH.

3.1.3. Thermogravimetric Analysis of PBS-LDH

Thermogravimetric analyses were performed in a two-step experiment, firstly in an inert atmosphere (Figure 2a), followed by an oxygen atmosphere heating (Figure 2b). The

neat PBS, Cl-LDH, and PBS-LDH were tested. PBS-LDH presented a slighter decomposition temperature than Cl-HDL in the range of 130–400 °C, followed by a rapid mass loss between 500 and 800 °C, which is in agreement with the decomposition steps seen for neat PBS. We confirmed the presence of the UV absorber by comparing the curves for PBS and PBS-LDH under an oxygen atmosphere.

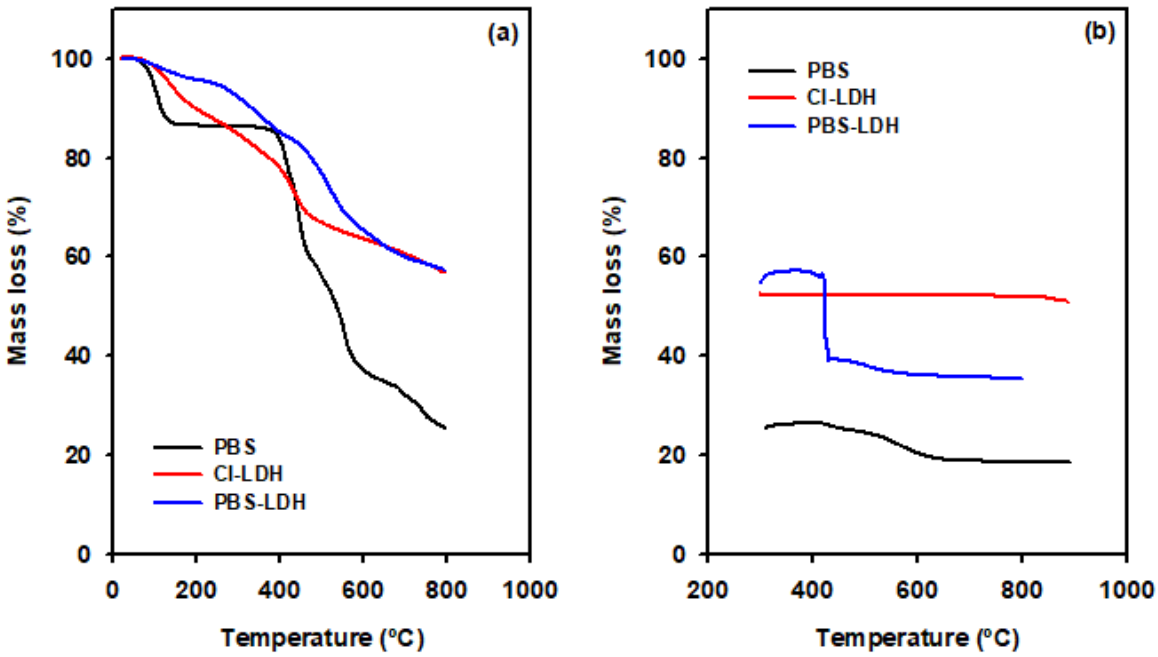

Figure 2. Thermogravimetric analysis of PBS, Cl-LDH, and PBS-LDH (**a**) under inert atmosphere and (**b**) subsequent oxidant atmosphere heating.

3.2. Characterization of the New Nanocomposites

Once the UV absorber and the dispersant agent had been incorporated into the LDH, this modified nanomaterial was added to LPDE to prepare films. Firstly, the samples were introduced in the compounding extruder and pelletized after the mixture. After that, the pellets were processed in the cast film extrusion line and films with a thickness of 200 microns were obtained. Four modified films were processed with a final concentration of PBS of 1 wt. %, either encapsulated in LDH or not. The addition of the dispersant agent SPAN and the neat LDPE was also studied. The concentrations of the additives are shown in Table 3.

Table 3. Films with the concentration of PBS-LDH, PBS, and/or SPAN.

		Concentration (wt. %)		
Sample	**LDPE**	**PBS-LDH**	**PBS**	**SPAN**
1	99	1	0	0
2	99	0	1	0
3	98	1	0	1
4	98	0	1	1
5	100	0	0	0

3.2.1. Optical Properties and UV-Aging Effect of the New Composites

The UV–visible spectra of the films are depicted in Figure 3. Fresh samples and aged films after 500 h were studied. The film with the highest transmission of light in the UV–visible range is neat PE. However, after 500 h in the ageing chamber, PE presented absorption in the UVB range (below 310 nm). This is an indicator of photodegradation, with the resulting chromophore groups able to absorb the radiation in the range of 200–310 nm [30].

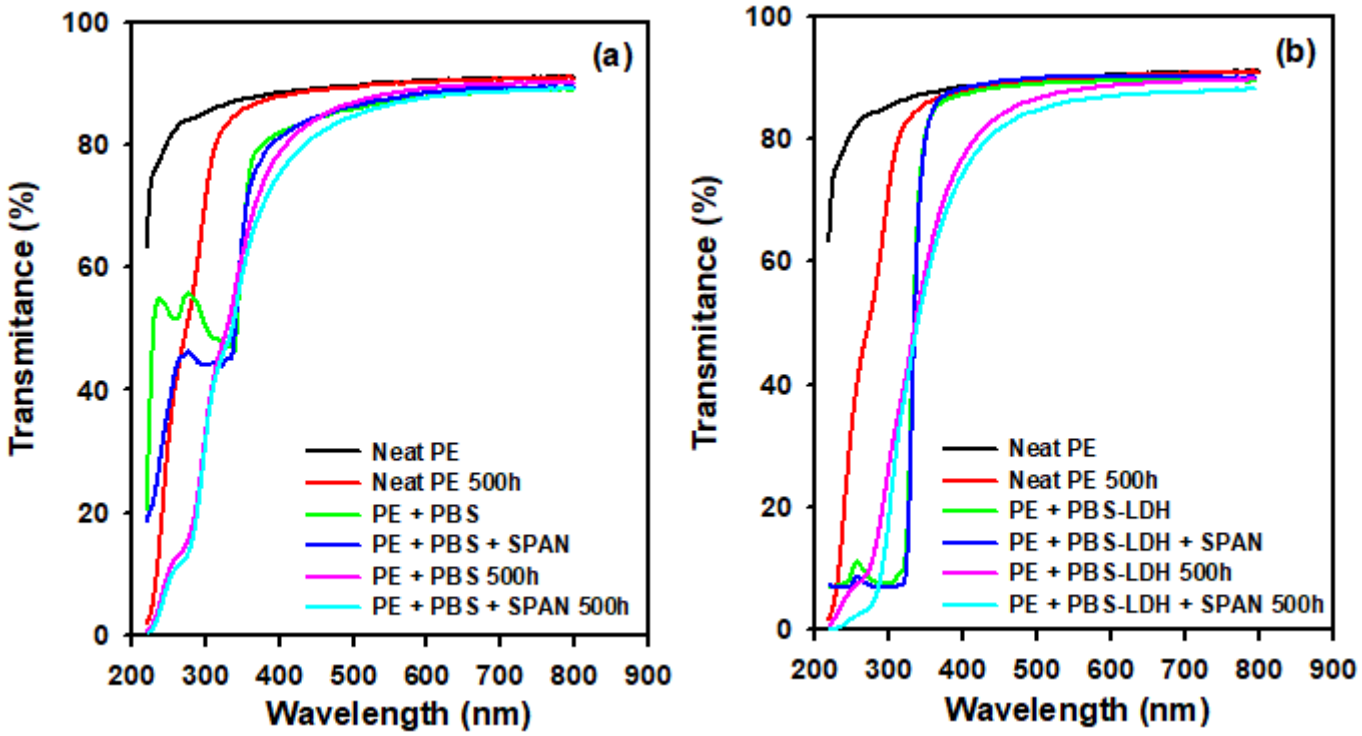

Figure 3. Effect of aging and addition of SPAN on the UV–vis spectra of (**a**) films with PBS and (**b**) PBS-LDH. Neat PE is also included in both graphs.

3.2.2. Mechanical and Rheological Properties and XRD Patterns of the New Films

We have performed tensile tests to evaluate the mechanical performance of these new composites compared to neat PE. The data relating to the elongation at break and the yield and tensile strengths when the stress was applied in the longitudinal and transversal directions of extrusion are presented in Figure 4. The longitudinal properties presented larger values due to the characteristic anisotropy of the material.

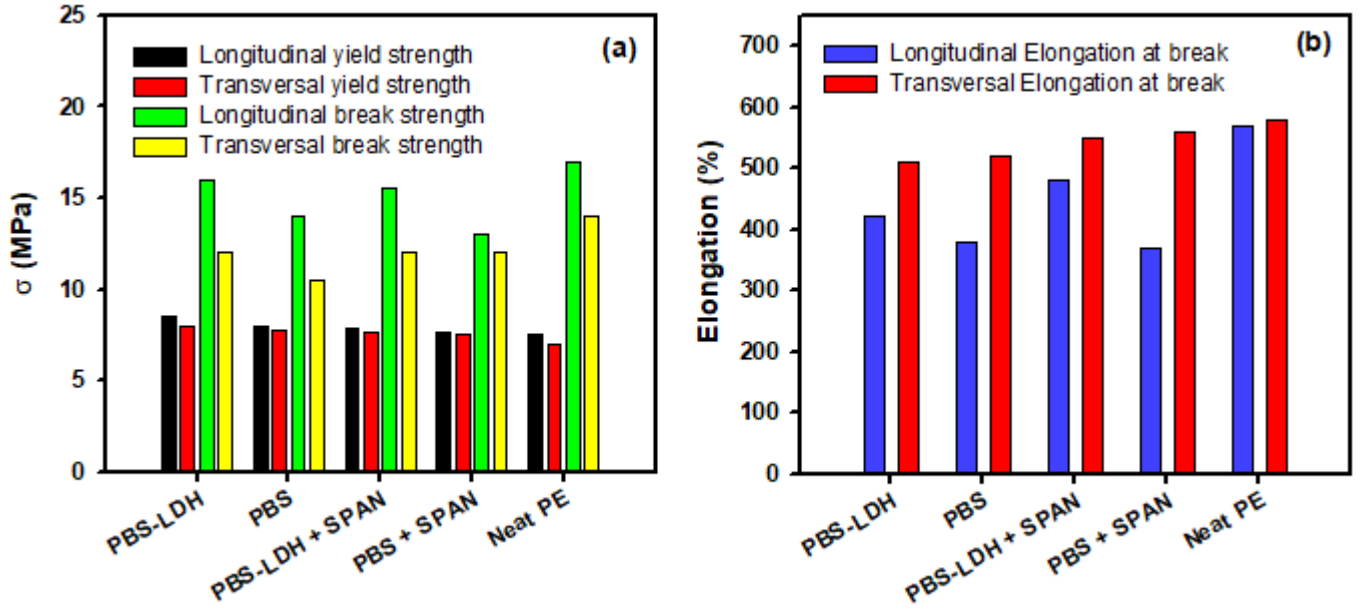

Figure 4. Mechanical properties of neat PE and modified films with PBS, PBS+SPAN, PBS-LDH, and PBS-LDH+SPAN. In (**a**), the strengths are represented; in (**b**), the nominal deformation when the load is applied in both the longitudinal and vertical directions of extrusion is represented.

The rheological data of the films at 190 °C are shown in Figure 5a. All tests were conducted under 1% of deformation, as was determined by the LVR conditions. The values of elastic modulus (G′) and viscous modulus (G″) are depicted for neat PE. At low frequencies, the viscous behavior prevailed over the elastic behavior. However, a crossing point was seen at circa 6 Hz. Therefore, the relaxation time was 0.17 s, as was calculated as the inverse of this cross-over. This is a characteristic value at which it is stated that the thermoplastic matrix is able to relax to a steady state due to the mobility of the polymeric chains [31]. This value remained almost constant for all the samples, probably because of the low concentration of additives.

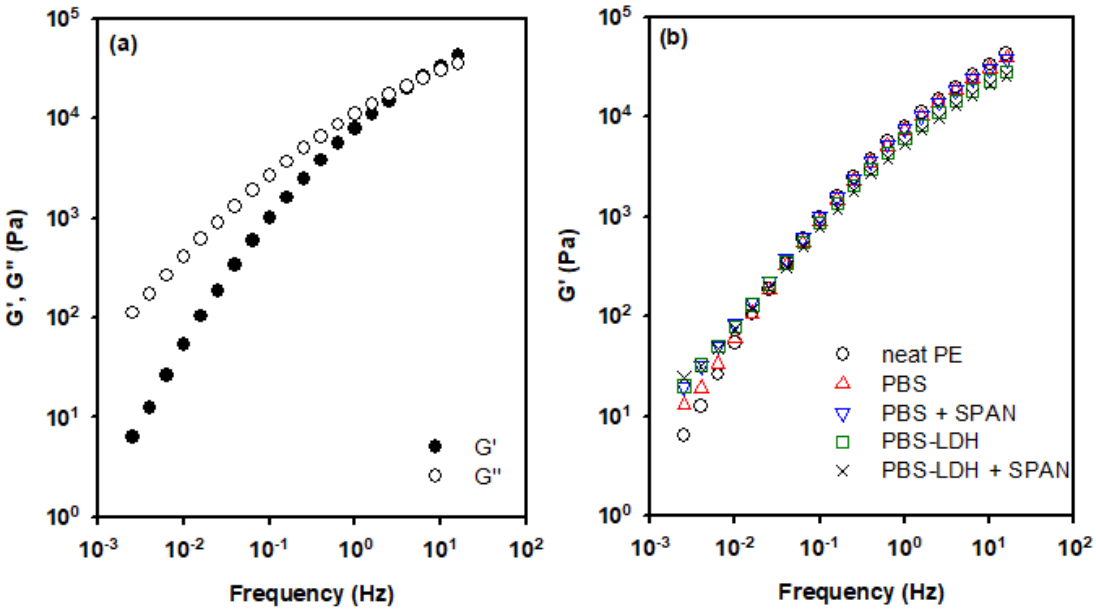

Figure 5. (**a**) Elastic (G′) and viscous (G″) moduli of neat PE and (**b**) influence of surfactant on the elastic modulus of films of PE, PE + PBS, and PE + PBS-LDH. Data at 190 °C.

XRD analysis of Cl-LDH, PBS-LDH, and the film including this additive are shown in Figure 6. When we compared the Cl-LDH with PBS-LDH, there was an increase in the basal d-spacing, and a shift in d003 and d006 peaks to lower values of 2θ was observed. Thus, there was an increase of the distance of the interlayers due to the replacement of chloride anions by PBS, in agreement with the FTIR and TGA data shown above. The figure also shows the PE film with PBS-LDH and the surfactant SPAN.

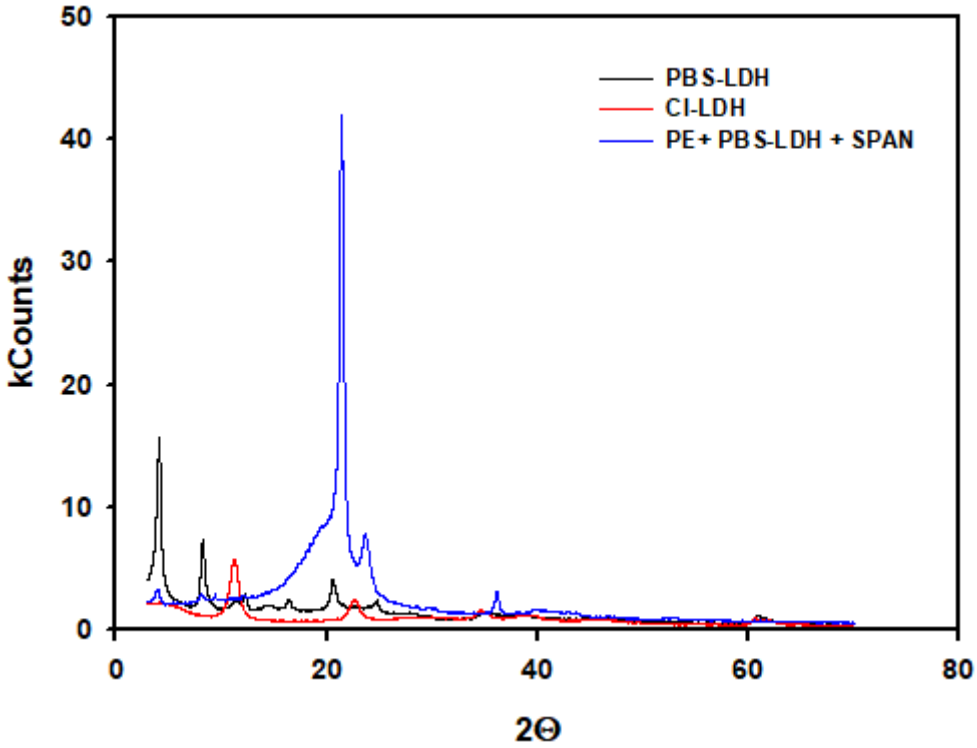

Figure 6. XRD diffractograms of original Cl-LDH, LDH modified with PBS, and the film with PBS-LDH and surfactant.

4. Discussion

A critical aspect of this study is the determination of the effectiveness of the encapsulation of PBS in the nanoclay. According to the XRF and CHS data shown in Table 2, the chloride content decreased, whilst the carbon content increased, indicating the replacement of Cl^- by PBS. Using these data, we calculated the value of x (molar ratio: $M_{III}/(M_{II} + M_{III})$) as 0.49, which means that a passive layer $Al(OH)_3$ is present, since the value is greater than 0.33 [32]. Therefore, the theoretical formula of PBS-LDH can be expressed as $Mg_{0.65}Al_{0.35}(OH)_2(PBS)_{0.35}{\cdot}0.68H_2O$, and the PBS content in LDH was 46.5 wt. % and 53.5 wt. % with the LDH. In the thermal analysis, a loss of pyrolytic carbon in PBS and the modified LDH was not seen in Cl-LDH (seen in Figure 2b). From these data, PBS-LDH presented with 35% inorganic remains, 51% in the case of Cl-LDH, and 18% in PBS. Using the XRF and CHS results, these inorganic remains can be theoretically calculated as (46.5 × 0.185) + (53.5 × 0.51) = 35%, consistent with TGA measurements. Therefore, there is an effective encapsulation of PBS in LDH.

It is worth noting that in comparing PBS and PBS-LDH, there was a thermal stabilization of the UV absorber when it was encapsulated. In Figure 2a, there is a first-step decomposition of PBS with a mass loss of 13.5% at 200 °C. On the other hand, PBS-LDH presents a mass loss of only 4% at the same temperature. Even taking into account that PBS-LDH is composed by only 46.5 wt. % of the sunscreen, the encapsulation in LDH avoids the thermal degradation of PBS at that temperature. As was described in Table 1, the extrusion profile of LDPE reaches 200 °C. Therefore, according to these data, PBS-LDH is a more suitable additive to be included in LDPE compared to neat PBS.

UV–visible spectrophotometry was used to evaluate the age-resistance effect of the addition of PBS and PBS-LDH on LDPE. The UV spectra when neat PBS was added indicate that this additive functioned as a UVB absorber below 330 nm (Figure 3). The acid form of PBS (2-Phenylbenzimidazole-5-sulfonic acid or PBSA) presented a strong activity at UVB (290–320 nm) wavelengths, attenuating the high-energy photons in sunlight [22,33]. Therefore, it is confirmed that PBS functioned as a UV absorber. On the other hand, when PBS was encapsulated in LDH, it is seen in Figure 3b that the UVB absorption of PBS

was enhanced (Figure 3b), as was the light transmission in the visible spectrum. PBS-LDH showed a much better thermal stability than PBS because the UV absorber in PE + PBS films could be partially degraded during the casting process and the sunscreen activity is enhanced in the encapsulated form. In this regard, the addition of PBS-LDH showed improved age-resistance and is a suitable option for outdoors applications such as fabrication of greenhouses [34], pipe coatings [35], or insulation [36].

Photodegradation of the film was also observed, and the presence of chromophore groups with UVB radiation activity could be an indicator of a pro-degrading effect of the additive [21,37]. This can be ascribed to the fact that PBS exhibits photosensitizing activity and generates reactive oxygen species [38]. Therefore, these films also showed photodegradation, and other UV stabilizers should probably be included in the formulation. In every case, the addition of the dispersant had no effect on the optical performance of the films.

Tensile tests were carried out to explore the effect of the additives on the composites' mechanical properties. Regarding the mechanical properties of the new films, the additives decreased the break strength of the composites (Figure 4a), mainly when SPAN was added, as expected. This decrease was more obvious in the transversal direction due to the lower directionality of the polymeric chains after extrusion [21]. Remarkably, the modified film with PBS-LDH presented the higher mechanical properties, indicating better interaction with the plastic. On the other hand, the yield strength was slightly improved in both the longitudinal and transversal directions when the additives were included. Figure 4b shows the values of the elongation at break. The modified films presented lower deformation than neat PE. Encapsulated PBS showed higher values of elongation, and the addition of surfactant improved the malleability of the films.

Viscoelastic analysis was used to evaluate the processability and the interaction of the additives with the polymeric matrix. The rheological data showed that the viscoelastic behavior of the melt nanocomposites is similar, and all the films can be easily obtained with the same extrusion conditions. Figure 5b shows a comparison of G' for neat PE, PE + PBS, and PE + PBS + SPAN, and the analogous encapsulated PBS sample is observed, at 190 °C. The addition of only PBS to PE did not affect the viscoelastic behavior of the film. On the other hand, the addition of PBS-LDH and/or SPAN enhanced the values of G' at low frequencies. This finding indicates that there was a higher interaction with the polymeric matrix when PBS was encapsulated and/or the surfactant was included in the formulation. Thus, the concentration of percolation was reached [15,39].

The good interaction between PBS-LDH and LDPE was also confirmed with the aid of XRD test. In a previous work, we determined the d-basal space of the original LDH as 7.60 Å. In Figure 6, we can see that the value of the d003 peak is shifted slightly from 21.48 in the case of PBS-LDH to 22.05 Å when it is added to LDPE. Analogously, d006 is shifted from 10.72 to 10.91 Å. Thus, there is an increase in the d-basal space of PBS-LDH when it is added to the thermoplastic. Considering that SPAN 60 is not an anionic surfactant, interactions with the polymer were not expected. Furthermore, this additive did not show any influence on either the optical or rheological properties. Thus, the increase of the d-basal space could be ascribed to larger spacing between interlayers because of the intercalation of the polymer chains [40,41] rather than an exfoliating effect of the additives in the nanoclay.

5. Conclusions

In this work, we evaluated the incorporation of an anionic UV absorber additive to LDPE films. By means of ion-exchange reaction, PBS acted as a counter anion in LDH nanoclay. FT-IR, XRF, CHNS, XRD, and TG analyses demonstrated the effective encapsulation of PBS in the interlayer of the hydrotalcite-like material. It was also observed that PBS-LDH presented higher thermal stability than PBS. The modified LDH was incorporated into LDPE films by simple cast extrusion. The UV–visible spectroscopy showed that the film with PBS-LDH presented higher values of UV absorption and higher transmission of visible

light than that with plain addition of PBS. This is due to the thermal degradation of PBS during the extrusion of the plastic, as observed in the TGA curves.

These films were artificially aged, and it seemed that PBS-LDH presented a pro-degrading effect on LDPE and the addition of UV stabilizers might be necessary. Minor effects of the additives on the mechanical properties of the films were found; however, it is worth noting that an increase in the yield strength was seen when the LDH was added to the formulation. This indicates a higher interaction with the polymeric matrix. The surfactant SPAN did not show significant effects on either the optical or the mechanical properties of the films, indicating that this additive might not be necessary for the new formulation. When the rheological properties were examined, very small changes were found in the viscoelasticity of the materials, denoting that the processing conditions of these composites were similar to neat LDPE. In comparing the XRD patterns of PBS-LDH and the film containing this additive, larger interlayer spaces were found. Therefore, this modified LDH showed a strong interaction with LDPE, and the polymeric chains were intercalated in the nanomaterial. However, complete exfoliation of the LDH was not observed.

In conclusion, the encapsulation of PBS in LDH is an excellent approach to use this additive as a sunscreen protector for polymeric matrices due to the enhancement of the thermal stability of the PBS and the better dispersibility on this non-polar material. The obtained composites showed favorable processability, good mechanical performance, and improved age resistance, with the potential to extend the resulting product's lifetime and reduce waste.

Author Contributions: Conceptualization, F.M. and R.P.; methodology, F.M. and A.A.; validation, F.J.C.-V., A.A. and R.P.; formal analysis, F.M. and R.P.; investigation, F.M. and A.A.; resources, F.J.C.-V. and R.P.; data curation, F.M., A.A. and R.P.; writing—original draft preparation, R.P.; writing—review and editing, F.M., F.J.C.-V., A.A. and R.P.; visualization, R.P.; supervision, F.J.C.-V. and R.P.; project administration, A.A. and F.J.C.-V.; funding acquisition, F.J.C.-V. and R.P. All authors have read and agreed to the published version of the manuscript.

Funding: The authors acknowledge the financial support of the Ministerio de Economía y Competitividad and Agencia Estatal de Investigación (MINECO and AEI, Spain), EU-FEDER (MAT2017-85130-P, and PID2021-122169NB), and the Fundación Seneca, Agencia de Ciencia y Tecnología de la Región de Murcia ("Ayuda a las Unidades y Grupos de Excelencia Científica de la Región de Murcia"; Grant # 19877/GERM/15).

Conflicts of Interest: The authors declare no conflict of interest.

References

1. Leroux, F.; Besse, J. Polymer interleaved layered double hydroxide: A new emerging class of nanocomposites. *Chem. Mater.* **2001**, *13*, 3507–3515. [CrossRef]
2. Bubniak, G.A.; Schreiner, W.H.; Mattoso, N.; Wypych, F. Preparation of a new nanocomposite of $Al_{0.33}Mg_{0.67}(OH)_2(C_{12}H_{25}SO_4)_{0.33}$ and poly(ethylene oxide). *Langmuir* **2002**, *18*, 5967–5970. [CrossRef]
3. Pereira, C.M.C.; Herrero, M.; Labajos, F.M.; Marques, A.T.; Rives, V. Preparation and properties of new flame retardant unsaturated polyester nanocomposites based on layered double hydroxides. *Polym. Degrad. Stab.* **2009**, *94*, 939–946. [CrossRef]
4. Du, L.; Qu, B.; Zhang, M. Thermal properties and combustion characterization of nylon 6/MgAl-LDH nanocomposites via organic modification and melt intercalation. *Polym. Degrad. Stab.* **2007**, *92*, 497–502. [CrossRef]
5. Mochane, M.J.; Magagula, S.I.; Sefadi, J.S.; Sadiku, E.R.; Mokhena, T.C. Morphology, Thermal Stability, and Flammability Properties of Polymer-Layered Double Hydroxide (LDH) Nanocomposites: A Review. *Crystals* **2020**, *10*, 612. [CrossRef]
6. Pamies, R. Polymer Rheology and Processing of Nano- and Micro-Composites. *Materials* **2022**, *15*, 7297. [CrossRef]
7. Cozzarini, L.; Benedetti, E.; Piras, A.; Terenzi, A.; Pricl, S.; Schmid, C. Mechanical and flammability properties of a polyamide 6,6 nanocomposite for nonstructural marine engine components. *J. Polym. Eng.* **2021**, *41*, 27–33. [CrossRef]
8. Zhao, H.; Nagy, K.L. Dodecyl sulfate-hydrotalcite nanocomposites for trapping chlorinated organic pollutants in water. *J. Colloid. Interface Sci.* **2004**, *274*, 613–624. [CrossRef]
9. Maziarz, P.; Matusik, J.; Leiviskä, T. Mg/Al LDH Enhances Sulfate removal and Clarification of AMD Wastewater in Precipitation Processes. *Materials* **2019**, *12*, 2334. [CrossRef]
10. Lerner, D.A.; Bégu, S.; Aubert-Pouëssel, A.; Polexe, R.; Devoisselle, J.-M.; Azaïs, T.; Tichit, D. Synthesis and Properties of New Multilayer Chitosan@layered Double Hydroxide/Drug Loaded Phospholipid Bilayer Nanocomposite Bio-Hybrids. *Materials* **2020**, *13*, 3565. [CrossRef]

11. Saha, C.; Ponnupandian, S.; Costa, F.R.; Heinrich, G.; Singha, N.K. Polydimethylsiloxane based polyurethane and its composite with layered double hydroxide: Synthesis and its thermal properties. *Polym. Eng. Sci.* **2021**, *61*, 3163–3169. [CrossRef]
12. Jaerger, S.; Wypych, F. Thermal and flammability properties influenced by Zn/Al, Co/Al, and Ni/Al layered double hydroxide in low-density polyethylene nanocomposites. *J. Appl. Polym. Sci.* **2020**, *137*, 48737. [CrossRef]
13. Machrouhi, A.; Taoufik, N.; Elhalil, A.; Tounsadi, H.; Rais, Z.; Barka, N. Patent Blue V Dye Adsorption by Fresh and Calcined Zn/Al LDH: Effect of Process Parameters and Experimental Design Optimization. *J. Compos. Sci.* **2022**, *6*, 115. [CrossRef]
14. Tsai, T.Y.; Bunekar, N.; Wu, T.C. The Role of Organomodified Different LDHs on Recycled Poly(ethylene terephthalate) Nanocomposites. *J. Chin. Chem. Soc.* **2017**, *64*, 851–859. [CrossRef]
15. Costa, F.R.; Wagenknecht, U.; Jehnichen, D.; Goad, M.A.; Heinrich, G. Nanocomposites based on polyethylene and Mg–Al layered double hydroxide. Part II. Rheological characterization. *Polymer* **2006**, *47*, 1649–1660. [CrossRef]
16. Zahra, S.; Abbas, S.S.; Mahsa, M.-T.; Mohsen, N. Biodegradation of low-density polyethylene (LDPE) by isolated fungi in solid waste medium. *Waste Manag.* **2010**, *30*, 396–401. [CrossRef]
17. Awasthi, S.; Srivastava, P.; Singh, P.; Tiwary, D.; Mishra, P.K. Biodegradation of thermally treated high-density polyethylene (HDPE) by Klebsiella pneumoniae CH001. *3 Biotech* **2017**, *7*, 332. [CrossRef]
18. Rajandas, H.; Parimannan, S.; Sathasivam, K.; Ravichandran, M.; Yin, L.S. A novel FTIR-ATR spectroscopy based technique for the estimation of low-density polyethylene biodegradation. *Polym. Test.* **2012**, *31*, 1094–1099. [CrossRef]
19. Tsala-Mbala, C.; Hayibo, K.S.; Meyer, T.K.; Couao-Zotti, N.; Cairns, P.; Pearce, J.M. Technical and Economic Viability of Distributed Recycling of Low-Density Polyethylene Water Sachets into Waste Composite Pavement Blocks. *J. Compos. Sci.* **2022**, *6*, 289. [CrossRef]
20. Dilara, P.A.; Briassoulis, D. Degradation and Stabilization of Low-density Polyethylene Films used as Greenhouse Covering Materials. *J. Agric. Eng. Res.* **2000**, *76*, 309–321. [CrossRef]
21. Monzo, F.; Caparros, A.V.; Perez-Perez, D.; Arribas, A.; Pamies, R. Synthesis and Characterization of New Layered Double Hydroxide-Polyolefin Film Nanocomposites with Special Optical Properties. *Materials* **2019**, *12*, 3580. [CrossRef] [PubMed]
22. Inbaraj, J.J.; Bilski, P.; Chignell, C.F. Photophysical and photochemical studies of 2-phenylbenzimidazole and UVB sunscreen 2-phenylbenzimidazole-5-sulfonic acid. *Photochem. Photobiol.* **2002**, *75*, 107–116. [CrossRef] [PubMed]
23. Shen, L. Photophysical and photosensitizing characters of 2-phenylbenzimidazole-5-sulfonic acid. A theoretical study. *Spectrochim. Acta Part A Mol. Biomol. Spectrosc.* **2015**, *150*, 187–189. [CrossRef]
24. Perioli, L.; Ambrogi, V.; Rossi, C.; Latterini, L.; Nocchetti, M.; Costantino, U. Use of anionic clays for photoprotection and sunscreen photostability: Hydrotalcites and phenylbenzimidazole sulfonic acid. *J. Phys. Chem. Solids* **2006**, *67*, 1079–1083. [CrossRef]
25. Iyi, N.; Matsumoto, T.; Kaneko, Y.; Kitamura, K. Deintercalation of carbonate ions from a hydrotalcite-like compound: Enhanced decarbonation using acid-salt mixed solution. *Chem. Mater.* **2004**, *16*, 2926–2932. [CrossRef]
26. Saravanabharathi, D.; Obulichetty, M.; Kumaravel, M. Facile crystallization of 2-phenyl benzimidazole-5-sulfonic acid: Characterization of lattice water dependent zwitterionic supramolecular forms, with modulation in proton conductivities. *J. Chem. Sci.* **2019**, *131*, 72. [CrossRef]
27. Shishlov, N.M.; Khursan, S.L. Effect of ion interactions on the IR spectrum of benzenesulfonate ion. Restoration of sulfonate ion symmetry in sodium benzenesulfonate dimer. *J. Mol. Struct.* **2016**, *1123*, 360–366. [CrossRef]
28. Langner, R.; Zundel, G. FTIR investigation of O center dot center dot center dot H center dot center dot center dot O hydrogen bonds with large proton polarizability in sulfonic acid-N-oxide systems in the middle and far-IR. *J. Chem. Soc. Faraday Trans.* **1998**, *94*, 1805–1811. [CrossRef]
29. Perpetuo, G.J.; Goncalves, R.S.; Janczak, J. Supramolecular hydrogen-bonding network in 1-(diaminomethylene)thiouron-1-ium 4-hydroxybenzenesulfonate crystal. *J. Mol. Struct.* **2015**, *1096*, 74–83. [CrossRef]
30. Kaczmarek, H.; Oldak, D.; Podgorski, A. Photochemical properties of polyethylene modified by low-molecular organic compounds. *Polym. J.* **2003**, *35*, 634–639. [CrossRef]
31. Georgantopoulos, C.K.; Esfahani, M.K.; Naue, I.F.C.; Wilhelm, M.; Kadar, R. Role of molecular architecture and temperature on extrusion melt flow instabilities of two industrial LLDPE and LDPE polyethylenes investigated by capillary rheology, high-pressure sensitivity slit die and optical analysis. *J. Appl. Polym. Sci.* **2022**, *40*, e53165. [CrossRef]
32. Solera, P. New trends in polymer stabilization. *J. Vinyl Addit. Technol.* **1998**, *4*, 197–210. [CrossRef]
33. Stevenson, C.; Davies, R.J.H. Photosensitization of guanine-specific DNA damage by 2- phenylbenzimidazole and the sunscreen agent 2-phenylbenzimidazole-5-sulfonic acid. *Chem. Res. Toxicol.* **1999**, *12*, 38–45. [CrossRef] [PubMed]
34. Battacharjee, L.; Jazaei, F.; Salehi, M. Insights into the mechanism of plastics' fragmentation under abrasive mechanical forces: An implication for agricultural soil health. *Clean Soil Air Water* **2023**, *51*, 2200395. [CrossRef]
35. Lim, J.; Kim, S.J. Fabrication and experimental evaluation of a polymer-based flexible pulsating heat pipe. *Energy Convers. Manag.* **2018**, *156*, 358–364. [CrossRef]
36. Hong, Z.; Chen, X.; Zhu, H.; Zhang, T.; Li, H.; Awais, M.; Paramane, A. Insulation properties enhancement of crosslinked polyethylene by grafting electron-buffering voltage stabilizers. *J. Appl. Polym. Sci.* **2023**, E54633. [CrossRef]
37. Lonkar, S.P.; Therias, S.; Caperaa, N.; Leroux, F.; Gardette, J.L. Photooxidation of polypropylene/layered double hydroxide nanocomposites: Influence of intralamellar cations. *Eur. Polym. J.* **2010**, *46*, 1456–1464. [CrossRef]

38. Bastien, N.; Millau, J.-F.; Rouabhia, M.; Davies, R.J.H.; Drouin, R. The sunscreen agent 2-phenylbenzimidazole-5-sulfonic acid photosensitizes the formation of oxidized guanines in cellulo after UV-A or UV-B exposure. *J. Investig. Dermatol.* **2010**, *130*, 2463–2471. [CrossRef]
39. Saritha, A.; Joseph, K. *Melt Rheological Properties of Layered Double Hydroxide Polymer Nanocomposites*; Woodhead Publishing: Sawston, UK, 2020. [CrossRef]
40. Lee, W.D.; Im, S.S.; Lim, H.M.; Kim, K.J. Preparation and properties of layered double hydroxide/poly(ethylene terephthalate) nanocomposites by direct melt compounding. *Polymer* **2006**, *47*, 1364–1371. [CrossRef]
41. Wang, L.J.; Su, S.P.; Chen, D.; Wilkie, C.A. Variation of anions in layered double hydroxides: Effects on dispersion and fire properties. *Polym. Degrad. Stab.* **2009**, *94*, 770–781. [CrossRef]